

# Increased activity of *Diaphanous homolog 3 (DIAPH3)*/ *diaphanous* causes hearing defects in humans with auditory neuropathy and in *Drosophila*

Cynthia J. Schoen<sup>a,b</sup>, Sarah B. Emery<sup>c</sup>, Marc C. Thorne<sup>c</sup>, Hima R. Ammana<sup>d</sup>, Elzbieta Śliwerska<sup>b</sup>, Jameson Arnett<sup>c</sup>, Michael Hortsch<sup>e</sup>, Frances Hannan<sup>d,f</sup>, Margit Burmeister<sup>b,g,h</sup>, and Marci M. Lesperance<sup>c,1</sup>

<sup>a</sup>Neuroscience Graduate Program, <sup>b</sup>Molecular & Behavioral Neuroscience Institute, <sup>c</sup>Division of Pediatric Otolaryngology, Department of Otolaryngology-Head and Neck Surgery, and Departments of <sup>e</sup>Cell and Developmental Biology, <sup>g</sup>Human Genetics, and <sup>h</sup>Psychiatry, University of Michigan Health System, Ann Arbor, MI 48109; and Departments of <sup>d</sup>Cell Biology and Anatomy and <sup>f</sup>Otolaryngology, New York Medical College, Valhalla, NY 10595

Edited\* by Mary-Claire King, University of Washington, Seattle, WA, and approved June 15, 2010 (received for review March 11, 2010)

**Auditory neuropathy is a rare form of deafness characterized by an absent or abnormal auditory brainstem response with preservation of outer hair cell function. We have identified *Diaphanous homolog 3 (DIAPH3)* as the gene responsible for autosomal dominant nonsyndromic auditory neuropathy (*AUNA1*), which we previously mapped to chromosome 13q21-q24. Genotyping of additional family members narrowed the interval to an 11-Mb, 3.28-cM gene-poor region containing only four genes, including *DIAPH3*. DNA sequencing of *DIAPH3* revealed a c.-172G > A, g.48G > A mutation in a highly conserved region of the 5' UTR. The c.-172G > A mutation occurs within a GC box sequence element and was not found in 379 controls. Using genome-wide expression arrays and quantitative RT-PCR, we demonstrate a 2- to 3-fold overexpression of *DIAPH3* mRNA in lymphoblastoid cell lines from affected individuals. Likewise, a significant increase ( $\approx 1.5$ -fold) in *DIAPH3* protein was found by quantitative immunoblotting of lysates from lymphoblastoid cell lines derived from affected individuals in comparison with controls. In addition, the c.-172G > A mutation is sufficient to drive overexpression of a luciferase reporter. Finally, the expression of a constitutively active form of diaphanous protein in the auditory organ of *Drosophila melanogaster* recapitulates the phenotype of impaired response to sound. To date, only two genes, the otoferlin gene *OTOF* and the pejvakin gene *PJVK*, are known to underlie nonsyndromic auditory neuropathy. Genetic testing for *DIAPH3* may be useful for individuals with recessive as well as dominant inheritance of nonsyndromic auditory neuropathy.**

genetics | 5'UTR | formin | overexpression | *DIAPH1*

**A**uditory neuropathy (AN) is a rare form of deafness resulting from a disorder of inner hair cells, their synapses with the auditory nerve (VIII nerve), or the auditory nerve itself, with preservation of outer hair cell function (1). In contrast, most forms of deafness are associated with a loss of outer hair cell function, as typically measured by otoacoustic emissions (OAEs). Although there are more than 60 genes for nonsyndromic deafness, the genetic architecture of nonsyndromic auditory neuropathy is not well understood. We now report the identification of *Diaphanous homolog 3 (DIAPH3)* as a gene responsible for a dominant form of nonsyndromic auditory neuropathy.

*DIAPH3* is one of three human orthologs of *Drosophila diaphanous*. A mutation in *DIAPH1* underlies *DFNA1*, autosomal dominant nonsyndromic sensorineural hearing loss (2), whereas mutations in the X-linked *DIAPH2* cause premature ovarian failure (3). These genes encode *diaphanous*-related formin (DRF) proteins, actin nucleation factors involved in maintenance of cell polarity and cell shape, intracellular transport, and vesicular trafficking (4). DRFs are maintained in an inactive state through an autoinhibitory interaction between the N-terminal GTPase-binding domain (GBD) and the C-terminal diaphanous autoinhibitory domain (DAD) (4). Binding of Rho-GTP to the GBD activates DRFs through displacement of DAD, a process which is tightly regulated.

We previously mapped the nonsyndromic auditory neuropathy, autosomal dominant 1 (*AUNA1*) locus to chromosome 13q21-q24 in an American family of European descent (5). Affected individuals in this family develop hearing loss in the second decade of life which rapidly progresses to profound deafness. Outer hair cell function as measured by OAEs is preserved until approximately the fifth decade of life. Electrically evoked responses of the auditory nerve return to normal after cochlear implantation, suggesting that the defect resides in the inner hair cells, the afferent synapses, or the terminal dendrites of the auditory nerve (6). Except for the possibility of slightly earlier onset in homozygotes, no phenotypic differences between homozygotes and heterozygotes were observed in this family.

## Results

Genotyping of additional short tandem repeat markers as well as single nucleotide polymorphisms in the linkage region refined the telomeric boundary of *AUNA1* to D13S1309, excluding the protocadherin 9 gene (*PCDH9*) (7). Genotyping of a DNA sample from a distantly related affected family member revealed a recombination event at marker D13S1492, which redefined the centromeric end of the *AUNA1* interval (Fig. S1). The refined *AUNA1* interval spans an 11-Mb, 3.28-cM genomic region containing only four genes: protocadherin 17 (*PCDH17*), protocadherin 20 (*PCDH20*), Tudor domain-containing 3 (*TDRD3*), and *DIAPH3*.

DNA sequencing of all exons and intron-exon junctions of *DIAPH3* demonstrated a point mutation in the 5' UTR, c.-172G > A, g.48G > A, occurring within a consensus GC box DNA recognition site (8). The 5' UTR DNA sequence is highly conserved in the vertebrate orthologs of the human *DIAPH3* gene (Fig. S2). The mutation is absent in 379 controls (758 control chromosomes), segregates with deafness, and, as predicted by the linkage analysis (5), is homozygous in two affected subjects. DNA sequencing of *PCDH17*, *PCDH20*, and *TDRD3* revealed no novel variants from the reference sequences.

Whole-genome expression arrays were used to identify genes that are differentially expressed in mRNA from lymphoblastoid cell lines (LCLs) from affected individuals and controls. Signal intensity was 2- to 3-fold higher in affected individuals than in controls for two probes representing the *DIAPH3* gene (*Hs. 576922* and *DIAPH3*;  $P = 0.000029$  and  $P = 0.000713$ , respectively). To confirm and

Author contributions: C.J.S., S.B.E., M.H., F.H., M.B., and M.M.L. designed research; C.J.S., S.B.E., M.C.T., H.R.A., E.S., J.A., M.H., F.H., M.B., and M.M.L. performed research; M.H., F.H., and M.B. contributed new reagents/analytic tools; C.J.S., S.B.E., M.C.T., E.S., M.H., F.H., M.B., and M.M.L. analyzed data; and C.J.S., S.B.E., M.H., F.H., M.B., and M.M.L. wrote the paper.

The authors declare no conflict of interest.

\*This Direct Submission article had a prearranged editor.

<sup>1</sup>To whom correspondence should be addressed. E-mail: lesperan@umich.edu.

This article contains supporting information online at [www.pnas.org/lookup/suppl/doi:10.1073/pnas.1003027107/-DCSupplemental](http://www.pnas.org/lookup/suppl/doi:10.1073/pnas.1003027107/-DCSupplemental).

quantify the expression changes seen on microarrays, the threshold cycle (Ct) for *DIAPH3*, as compared with the Ct for a housekeeping gene,  $\beta$ -glucuronidase (*GUSB*), was determined for controls, heterozygotes, and homozygotes by quantitative RT-PCR of mRNA from LCLs. The estimated difference of marginal means for  $\Delta C$  (Ct *GUSB* – Ct *DIAPH3*) was significant for controls vs. heterozygotes ( $-0.4285$  vs.  $0.6496$ ,  $P = 0.0028$ ) and controls vs. homozygotes ( $-0.4285$  vs.  $1.1466$ ,  $P < 0.001$ ) (Fig. 1). Expression was increased 2.11-fold in heterozygotes compared with controls and 2.98-fold in homozygotes compared with controls, as reflected by an increase in  $\Delta C$  values (Fig. 1). Results for homozygotes were not significantly different from those for heterozygotes ( $P = 0.2641$ ).

To determine the effect of increased mRNA expression on levels of protein expression, we used immunoblotting to compare relative amounts of DIAPH3 protein in LCL lysates from controls, heterozygotes, and homozygotes (Fig. 2A). GAPDH was used as a loading control, and the DIAPH3/GAPDH ratio was calculated. There was a significant difference in the estimated marginal means for the DIAPH3/GAPDH ratio in controls vs. heterozygotes ( $4.83$  vs.  $7.14$ ,  $P = 0.045$ ) and controls vs. homozygotes ( $4.83$  vs.  $7.85$ ,  $P = 0.0093$ ) (Fig. 2B). Protein levels were increased 1.48-fold in heterozygotes and 1.62-fold in homozygotes relative to controls (Fig. 2B). There was no significant difference in protein levels between homozygotes and heterozygotes ( $P = 0.68$ ).

Given the increased expression of *DIAPH3* observed in mRNA from affected family members, we investigated whether increased expression could be explained by the presence of the 5' UTR mutation. Although promoter and/or enhancer sequences for *DIAPH3* have not yet been identified, we hypothesized that the 5' UTR sequence plays a role in controlling the expression of *DIAPH3*. Therefore, the putative promoter and the 5' UTRs (mutant and wild-type) were cloned into a luciferase reporter vector to determine the effect of the c.-172G > A mutation on gene expression. When compared to the wild-type *DIAPH3* 5' UTR, the c.-172G > A mutation up-regulates the expression of a luciferase reporter gene significantly,  $\approx 2$ - to 3-fold ( $P < 0.001$ ) (Fig. 3). These data show that the c.-172G > A mutation is sufficient to cause the observed overexpression of *DIAPH3*.

Additional investigations of *DIAPH3* were performed to determine whether variations in splicing, differential abundance of normal transcripts, and/or novel transcripts caused by exon-skipping or rearrangements accounted for the observed change in *DIAPH3* expression. Comparison of PCR products spanning the *DIAPH3* cDNA shows no discernable difference in size or sequence varia-

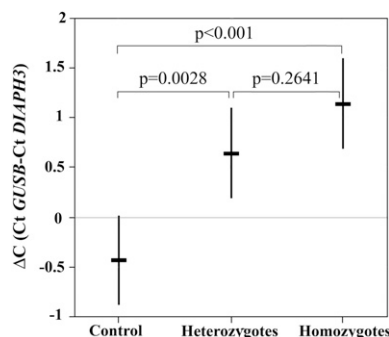


**Fig. 1.** *DIAPH3* is significantly overexpressed in mRNA from heterozygotes and homozygotes as compared with controls. Relative *DIAPH3* gene expression in mRNA extracted from LCLs of wild-type, homozygous, and heterozygous individuals was assessed using quantitative RT-PCR amplifying exons 19–20. The *DIAPH3* Ct was normalized to the Ct of the housekeeping gene *GUSB* to determine  $\Delta C$  (Ct *GUSB* – Ct *DIAPH3*) for each sample. Estimated marginal means for  $\Delta C$  (control =  $-0.4285$ ; heterozygotes =  $0.6496$ ; homozygotes =  $1.1466$ ) are indicated by bold horizontal lines, with 95% confidence intervals represented by vertical lines.  $P$  values for significance of difference of marginal means are indicated by brackets.

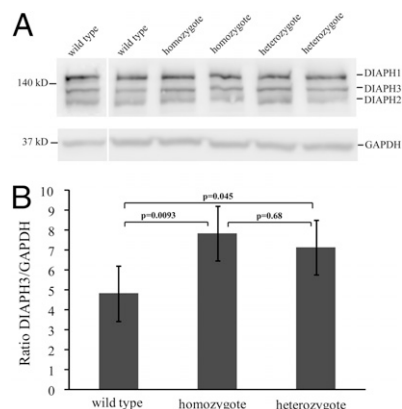


**Fig. 2.** Expression of DIAPH3 protein is significantly increased in lysates from LCLs from heterozygotes and homozygotes vs. controls. (A) Immunoblot of LCL lysates from two wild types, two homozygotes, and two heterozygotes using DT154 antibody (43, 44). The DIAPH3 band is at 137 kDa (UniProt database); cross-reactivity is seen with DIAPH1 (140 kDa) and DIAPH2 (126 kDa). GAPDH was used as a loading control, and DIAPH3 densitometry was normalized to GAPDH densitometry. (B) Estimated marginal means and SE for the DIAPH3/GAPDH ratio for wild types, homozygotes, and heterozygotes tested in four batches of cells. There was a significant difference between controls and heterozygotes ( $4.83$  vs.  $7.14$ ,  $P = 0.045$ , a 1.48-fold increase) and between controls and homozygotes ( $4.83$  vs.  $7.85$ ,  $P = 0.0093$ , a 1.62-fold increase). There was no significant difference in protein levels between homozygotes and heterozygotes ( $P = 0.68$ ).

tions between homozygote and control cDNA. Similarly, Northern blots show no novel transcripts in samples from affected individuals (Fig. S3). Finally, there was no difference in the relative abundance of any of the various *DIAPH3* transcripts in RNA from mutant LCLs as compared with controls (Fig. S4).

To investigate the role of diaphanous proteins in the auditory function of a model organism, we created lines of flies (*Drosophila melanogaster*) which express a constitutively active form of diaphanous protein in the auditory organ (Johnston's organ, JO). Sound-evoked potentials (SEPs) were compared in affected flies versus parental and wild-type control flies. We used five different JO-Gal4 lines, each with a specific expression pattern in the JO (Table S1). In the Gal4-upstream activating sequence (UAS) system, the yeast transcription activator protein Gal4 binds to the UAS to activate transcription of the transgene in a tissue- and temporally specific manner (9). UAS-diaphanous<sup>CA</sup> (UAS-diaCA) is a transgenic line which, in the presence of Gal4, expresses a mutant form of diaphanous protein, diaphanous<sup>CA</sup> (10). Diaphanous<sup>CA</sup> was created by removing both the N-terminal Rho-binding domain and the C-terminal autoinhibitory domain of *Drosophila* diaphanous (10); the lack of these regulatory domains results in a constitutively active protein. Expression of diaphanous<sup>CA</sup> under control of the JO1-Gal4 driver was found to be lethal in the late pupal stage and semilethal for the JO2-Gal4 driver line, with only a few viable flies.

For the four crosses generating viable flies, all those expressing diaphanous<sup>CA</sup> exhibit significantly reduced SEPs in comparison with wild-type flies and parental control flies (Fig. 4 and Table S2). The majority of responses of the wild-type flies and parental control flies fall in the range of 0.5–1.3 mV, whereas most flies with constitutive expression of diaphanous<sup>CA</sup> exhibit responses in the range of 0.25–0.75 mV.

## Discussion

We have identified a point mutation in the 5' UTR of the human *DIAPH3* gene that leads to overexpression of *DIAPH3* and causes a progressive nonsyndromic auditory neuropathy, *AUNAI*. The c.-172G > A substitution occurs within a GC box element con-

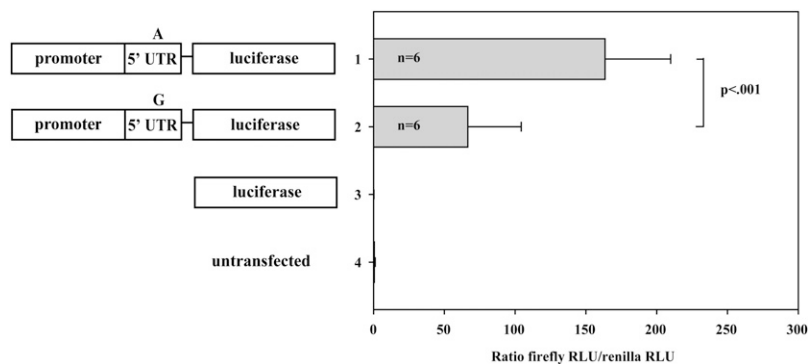


**Fig. 3.** Effect of base substitution in *DIAPH3* 5' UTR on luciferase reporter gene expression. (Left) Three constructs of the pGL3-basic luciferase reporter vector were tested, as were nontransfected cells: (1) promoter with mutant 5' UTR (c.-172G > A) from affected homozygote; (2) promoter and wild-type 5' UTR from CEPH DNA NA10846 (Coriell Cell Repositories); (3) no promoter or UTR; (4) untransfected cells. (Right) Normalized luciferase units are shown as mean  $\pm$  SD with  $n = 6$ . Expression from construct of DNA from affected individuals with mutant 5' UTR (line 1) is significantly higher than that of the wild-type 5' UTR (line 2) (unpaired  $t$  test,  $P < 0.001$ ). No expression was seen in construct lacking promoter and 5' UTR (line 3) or in untransfected cells (line 4).

sensus sequence (Fig. S2) known to bind transcription factors of the Sp1 and Krüppel-like protein families, which may function either as activators or repressors (11). We demonstrate that the mutant 5' UTR is sufficient to drive overexpression in a luciferase reporter vector, suggesting that this highly conserved sequence in the 5' UTR of *DIAPH3* may be important for its transcriptional regulation. Similar mutations in the 5' UTR of the  $\beta$ -globin gene have been shown to result in thalassemia through a reduction of mRNA levels (12, 13). Given the observed effect of overexpression, we postulate that the c.-172G > A mutation may decrease the binding of a transcriptional repressor. Other transcriptional mechanisms are possible, such as disruption of an internal ribosome entry site (14), increased binding of an activator, modification of the mRNA secondary structure, or alteration of microRNA binding.

A paralog of *DIAPH3*, *DIAPH1*, is responsible for *DFNA1* deafness, an autosomal dominant, progressive, low-frequency, sensorineural hearing loss (2). A G  $\rightarrow$  T substitution in a splice junction leads to a four-base insertion (TTAA), generating a frameshift that truncates the C terminus of the *DIAPH1* mRNA (2). Given the proximity of the truncation to the C-terminal DAD domain, it has been suggested that the *DFNA1* mutation interferes with auto-regulation of *DIAPH1* (15), resulting in a constitutively active protein. A knockout model of the mouse ortholog, *mdial1*, develops a myelodysplastic syndrome but has no apparent hearing defects (16). Thus, although the exact mechanism of *DFNA1* hearing loss is still unknown, a gain of function appears more likely than a loss-of-function mechanism such as haploinsufficiency.

Similar to *DIAPH1* deafness, our data support a gain-of-function mechanism causing *AUNAI* deafness by the overexpression of *DIAPH3*. Gain-of-function mechanisms of dominance include increased gene dosage, increased and/or constitutive activity of the protein, and ectopic or temporally altered mRNA expression (17). In LCLs, we demonstrate a significant 2- to 3-fold increase in mRNA expression over wild type by quantitative RT-PCR and an increase in protein levels of  $\approx 1.5$ -fold by immunoblotting. Although *DIAPH3* is ubiquitously expressed, family members with the c.-172G > A mutation do not develop clinical manifestations other than delayed-onset, rapidly progressive profound deafness. The human auditory system may be specifically sensitive to a 1.5-fold increase in *DIAPH3* protein levels, or the 2- to 3-fold increase in mRNA expression may be amplified to a greater degree at the protein level in the inner ear. Alternatively, the c.-172G > A mutation may lead to a constitutively active protein, augmenting *DIAPH3* activity beyond that expected from a mild increase in protein levels. Interestingly, a similarly modest (1.5- to 1.8-fold) level of overexpression in *MYO6*, a known deafness gene that is expressed in cochlear hair cells, also has been implicated in deafness (18).

Like *DIAPH1*, loss of function of *DIAPH3* is associated with neoplasia (19). In contrast, haploinsufficiency of the single *diaphanous* gene in *Drosophila* leads to an impaired response to sound (20). Redundant function of the three closely related DRF proteins in higher-order organisms such as humans and mice may

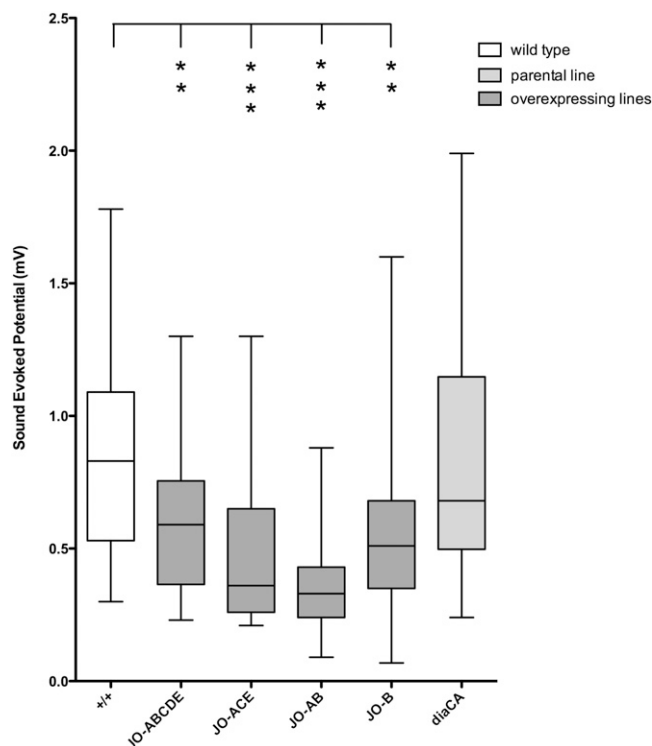


**Fig. 4.** Flies expressing a constitutively active diaphanous protein demonstrate impaired response to sound. Peak amplitude of SEP is reduced in flies expressing UAS-diaphanous<sup>CA</sup> in the JO auditory neurons (subgroups A, B, C, D, and/or E, as noted), (dark shaded bars) as compared with wild-type flies (++, unshaded bar) and diaphanous<sup>CA</sup> parental control flies (light shaded bar). Box plots indicate median, 25<sup>th</sup>, and 75<sup>th</sup> percentiles and minimum-maximum whiskers. The majority of responses of wild-type flies and parental control flies fall in the range of 0.5–1.3 mV. In contrast, most flies with constitutive overexpression of diaphanous protein exhibit responses in the range of 0.25–0.75 mV. SEPs are considerably lower in flies expressing diaphanous<sup>CA</sup> than in wild-type flies (\*\* $P < 0.005$ ; \*\*\* $P < 0.0001$ ; Mann-Whitney test) and in parental control flies (Table S2). Complete genotypes and expression patterns are shown in Table S1.

account for decreased sensitivity of the auditory organs to the lack of *DIAPH1* and *mdia1*, respectively (21). Knockdown of the zebrafish ortholog of *DIAPH3*, *zdia2*, by antisense morpholino oligonucleotides is lethal to the embryo before the formation of the auditory organ (22).

Formins are important in regulation of actin polymerization through effects on nucleation, elongation, and capping (23). In addition to coordination of actin dynamics, DRF proteins play a role in binding and regulating microtubules (24). In *Drosophila*, *diaphanous* is essential for the regulation of the presynaptic actin and microtubule cytoskeletons at the larval neuromuscular junction (25). In the cochlea, through their interaction with Rho GTPases, DRF proteins may play a role in specifying the precise shape and polarity of hair cell bundles (26) or in regulating stereocilia length mediated by the treadmilling mechanism (27). However, an abnormality of the stereocilia and/or bundles might be expected to affect inner and outer hair cells equally.

Alternatively, *DIAPH3* overexpression may cause deafness through a direct effect on the inner hair cell synapse. Approximately 95% of afferent auditory nerve fibers innervate mammalian inner hair cells, whereas only 5% of afferents innervate the outer hair cells (28). A recent study of mouse cortical and hippocampal neurons found that mDia2, the protein encoded by the gene orthologous to *DIAPH3*, is necessary for the function of dendritic spines, actin-rich structures arising from dendrites that house the post-synaptic components of excitatory synapses (29). Thus, a defect in afferent auditory nerve fibers might be expected initially to have a greater effect on inner hair cells but over time eventually would affect outer hair cells as well.

We created *Drosophila* models of constitutively active diaphanous protein expressed in the auditory organ (the JO) that replicate the phenotype of hearing loss. Because *Drosophila* has only one *diaphanous* gene, these crosses serve as models for gain-of-function mutations in both *DIAPH3* and *DIAPH1*. The JO consists of an array of mechanosensory neurons that share many developmental and functional similarities with mammalian inner hair cells (30, 31). There are five neuronal subgroups in the JO: neurons of subgroups A and B are activated by sound vibrations and are essential for hearing, whereas neurons in subgroups C and E respond to gravity and wind movements (32, 33). The function of neurons in subgroup D is currently unknown.

Each of the JO-Gal4 lines used in our experiments expresses in about 30–60% of the total population of JO neurons, including both A and B neurons (Table S1) (34). The lethality of the JO1-Gal4/*diaphanous*<sup>CA</sup> cross and the semilethality of the JO2-Gal4/*diaphanous*<sup>CA</sup> cross cannot be explained by their expression pattern in the JO but presumably are caused by expression in the *Drosophila* CNS outside the JO. Qualitatively, the JO1-Gal4 line drives a higher level of CNS expression than do the JO2-Gal4, JO3-Gal4, or JO4-Gal4 lines, and JO15-Gal4 has no detectable expression outside the JO (34).

The effect of expression of constitutively active diaphanous<sup>CA</sup> in neurons essential for hearing in *Drosophila* leads to a statistically significant reduction in response to sound in all four crosses yielding viable flies ( $P < 0.005$  for JO-3 and JO-2,  $P < 0.0001$  for JO-4 and JO-15; Fig. 4). The range of SEPs obtained from wild-type and parental control flies overlapped with those obtained from flies expressing diaphanous<sup>CA</sup>, largely because of a greater variability of hearing responses in the control flies. This variability has been observed previously (20, 32, 33) and may result in part from the technical limitations of placing the electrode in a consistent location within the JO. In contrast, uniformly low response levels were observed in the affected flies, in particular the JO15-Gal4 cross, which has expression limited to the auditory system (subgroups A and B of the JO neurons).

Only two genes, the otoferlin gene *OTOF* (35) and pejvakín *PJVK* (36), have been implicated previously in human nonsyndromic auditory neuropathy. *OTOF* originally was identified as the cause of

*DFNB9* recessive deafness (37) and appears to be a relatively common cause of recessive AN and sensorineural deafness in patients of Spanish descent (38, 39). Mutations in *PJVK* are reported in consanguineous families of Iranian descent, presenting either as autosomal recessive auditory neuropathy (*DFNB59*) (36) or sensorineural hearing loss (40). Auditory neuropathy may be unrecognized if testing is not performed early in life, because  $\approx 20$ –30% of AN subjects ultimately demonstrate loss of outer hair cell function over time (41). Furthermore, OAE testing is not performed routinely in all patients with significant hearing loss. Thus, it is difficult to estimate the proportion of cases of auditory neuropathy caused by mutations in these genes.

Elucidation of the role of the diaphanous-related formins in the cochlea may provide insights into the biology of these proteins as well as into the mechanisms underlying delayed-onset hearing loss. In addition, the discovery of *DIAPH3* as an auditory neuropathy gene will facilitate genetic testing for individuals with dominant and recessive auditory neuropathy.

## Methods

**Human Subjects.** Informed consent was obtained from participants, and studies were approved by the Institutional Review Board of the University of Michigan Medical School. DNA was extracted from peripheral venous blood samples and/or saliva. EBV transformation of peripheral lymphocytes was performed to create LCLs. RNA was isolated from LCLs with RNeasy Plus Mini Kit (QIAGEN). DNA samples not previously available were genotyped for markers linked to the *AUNA1* locus as described (5). All sequencing and genotyping was performed using dye-terminator cycle sequencing on a 3730xl DNA analyzer (Applied Biosystems) at the University of Michigan DNA Sequencing Core.

**Gene Expression Analysis.** Total RNA was isolated from LCLs derived from five control subjects and four affected family members (two homozygotes and two heterozygotes) and was prepared and hybridized to Illumina Human-6 v2 Expression BeadChips (Illumina, Inc) per the manufacturer's instructions. The chip was scanned on an Illumina BeadStation using Bioinformatics software, and data were downloaded to Illumina BeadStudio.

**DNA and cDNA Sequencing of *DIAPH3*.** Primers for PCR were designed to amplify *DIAPH3* cDNA and all exons and intron–exon junctions for DNA. For cDNA, reverse transcription was done with SuperScript III First Strand Synthesis Supermix (Invitrogen) on LCL RNA from a homozygote and from controls, using the manufacturer's recommended conditions for random hexamers. PCR was done with Failsafe (Epicenter Biotechnologies) according to the manufacturer's instructions. Sequence data were compared with the *DIAPH3* reference sequence NM\_001042517 with Lasergene software (DNASar).

Detected variants were screened using a custom probe (Custom TaqMan SNP Genotyping Assay; Applied Biosystems) or by DNA sequencing in 379 DNA samples (758 chromosomes) from controls consisting of 2 from unrelated spouses, 90 from the DNA Polymorphism Discovery Resource, 200 from the Caucasian Panel, and 87 from Human Variation Panels (10 Northern European, 10 Czechoslovakia, 10 African American, 10 South American, 9 Chinese, 10 Mexican, 10 Southeast Asian, 2 Middle Eastern, 9 South Saharan, and 7 Ashkenazi samples) (Coriell Cell Repositories).

**Multiple Sequence Alignment.** A multiple sequence alignment of the region that maps to the 5' end of a variety of orthologs for the human *DIAPH3* gene was performed with the Multiple Alignment based on Fast Fourier Transform (MAFFT) program (42). The analysis was limited to vertebrate species, which have 3 *diaphanous* genes.

**Quantitative RT-PCR.** A probe and primer set was selected for *DIAPH3* exons 19–20 from existing Taqman Gene Expression Assays (Applied Biosystems). Samples included RNA from LCLs of two heterozygotes, two homozygotes, and two controls. Cells were grown three times, and each batch was tested at four RNA concentrations (150, 125, 100, and 75 ng of RNA) in triplicate.

Real-time PCR was done with Taqman FAM-labeled MGB probe and primer sets (Applied Biosystems) on a 7900HT Fast Real-Time PCR System using the manufacturer's recommended conditions. *GUSB* was selected from a panel of endogenous controls (Applied Biosystems). Sequence Detection Systems 2.2.1 software (Applied Biosystems) was used to determine threshold cycle. The *DIAPH3* Ct was normalized to the Ct of the housekeeping gene *GUSB* to determine  $\Delta C$  (Ct *GUSB* – Ct *DIAPH3*) for each individual. The marginal mean for

$\Delta C$  with a 95% confidence interval was estimated and compared for homozygotes, heterozygotes, and controls. Fold change was calculated by raising 2 to the power of the difference ( $\Delta C$  controls –  $\Delta C$  homozygotes or heterozygotes).

**Protein Electrophoresis and Immunoblotting.** Four batches of LCLs, each consisting of two heterozygotes, two homozygotes, and two controls, were cultured for 2–3 wk, and lysate was prepared in RIPA buffer containing HALT protease inhibitor mixture (Thermo Scientific). Equal amounts of protein (50–100  $\mu$ g per batch) were electrophoresed on 4–20% gradient Tris•HCl-ready gels (Bio-Rad) and transferred to PVDF membranes (GE Healthcare Biosciences). Blots were blocked with 5% nonfat dry milk in TBS-T (Tris-buffered saline/0.1% Tween-20, pH 8). For DIAPH3, we used primary antibody DT154 at a dilution of 1:2,000 (43, 44); the secondary antibody was HRP-conjugated antibody against rabbit IgG diluted 1:10,000 (NA934V; GE Healthcare). Reactions were visualized using Supersignal West Femto Maximum Sensitivity Substrate (Thermo Scientific) and FluorChem SP imager (Cell Biosciences). Blots were stripped with Restore Western Blot Stripping Buffer (Thermo Scientific) and reprobed with primary antibody GAPDH (sc-25778; Santa Cruz Biotechnology) at a dilution of 1:1,000 using the same secondary antibody and Pierce ECL Western Blotting Substrate (Thermo Scientific).

Chemiluminescent detection was done on an Alpha Innotech imager (Cell Biosciences), and densitometry measurements for DIAPH3 and GAPDH were done with Alpha Ease software (Cell Biosciences). DIAPH3 measurements were normalized to bands detected by GAPDH in the sample to account for variability in amount loaded. The marginal mean for the ratio of DIAPH3/GAPDH was estimated, and fold change was calculated by dividing the estimated mean for homozygotes or heterozygotes by the estimated mean for wild type.

**Northern Blotting.** Poly(A)<sup>+</sup> RNA was isolated from the LCLs of two controls, two heterozygotes, and two homozygotes using the Dynabeads mRNA Direct Kit (Invitrogen). An RNA probe amplified from *DIAPH3* exon 28 was labeled using the DIG Northern Starter Kit (Roche Applied Science). *GAPDH* was used as a control probe.

**Sequence Analysis of Minor Transcription Products from *DIAPH3* Exons 1–5.** Total RNA prepared from the LCLs of one homozygote, two heterozygotes, and one unaffected individual was reverse transcribed using a combination of oligo (dT)<sub>20</sub> and random hexamer primers and SuperScriptase II (Invitrogen). To amplify the minor transcripts preferentially, the cDNA template was digested before PCR with *SspI* (New England Biolabs).

**Luciferase Assay. Reporter constructs.** A 256-bp region 21 bp upstream from the start of *DIAPH3* was identified as a putative promoter with PROSCAN Version 1.7 software (45). DNA from a homozygous affected individual (IV:9) (5) and a Centre d'Etude du Polymorphisme Humain (CEPH) control DNA (NA10846, Coriell Cell Repositories) were used as templates. For reporter constructs, PCR primers were designed to amplify the 256-bp putative promoter, the 21-bp linking region, and the 5' UTR of *DIAPH3*, with a *NheI* site in the forward primer and a *HindIII* site in the reverse primer. PCR was done using Failsafe reagents (Epicentre Biotechnologies) per the manufacturer's instructions and standard thermocycling conditions including an annealing temperature of 58 °C and 1 min extension for 32 cycles. The PCR product was isolated by agarose gel electrophoresis and purified with the MinElute Gel Extraction Kit (QIAGEN).

Purified PCR products and pGL3-basic firefly luciferase reporter vector (Promega) were digested with *NheI* and *HindIII* (New England Biolabs) and isolated and purified as outlined above. Vector and product were ligated with the Rapid DNA Ligation Kit (Roche) per the manufacturer's instructions

and transformed into *Escherichia coli* DH5 $\alpha$ -competent cells (Invitrogen). Plasmid preps for all three reporter constructs, pGL3-basic firefly luciferase reporter vector, and pRL-TK renilla luciferase control vector were done with the Qiaprep Spin Miniprep Kit (QIAGEN).

**Transfection.** For transfection,  $1.2 \times 10^5$  NIH 3T3 cells were seeded in each well of a 24-well plate and cultured overnight in fully supplemented DMEM (Gibco). Cells were washed twice and then covered with 500  $\mu$ L of DMEM without serum or antibiotics. A transfection mixture containing 100  $\mu$ L OptiMEM, 1.1  $\mu$ g of pGL3 firefly luciferase reporter construct or vector, 0.1  $\mu$ g of pRL-TK renilla luciferase reporter vector (Promega), and 2.6  $\mu$ L of lipofectamine 2000 (Invitrogen) was made per the manufacturer's protocol and added to each well for a 4-h incubation at 37 °C. Transfection medium was replaced with fully supplemented DMEM, and cells were grown for 20 h. Cells were washed with PBS, and luciferase activity was determined for firefly and renilla luciferase using the Dual Luciferase Assay kit and the GloMax 96 Microplate Luminometer (Promega).

***Drosophila melanogaster* Studies.** The expression pattern in the JO for the various JO-Gal4 driver lines used is described in Table S1. All flies were outcrossed for 5–10 generations to an isogenized line of wild-type control flies (*w*<sup>118(isoCJ1)</sup>). JO15/TM3Ser flies were constructed using standard genetic crosses. Flies were raised on sucrose/cornmeal medium at 25 °C on a 12-h light/dark cycle.

Recordings of SEPs were made from the antennae of female mutant and control flies as described previously (20). Control flies included wild-type (+/+) as well as parental control flies (UAS-diaphanous<sup>CA/+</sup>, and JO-Gal4/+). Twenty to 30 flies of each genotype were assayed in a blind fashion. Responses to 10 stimulus presentations were averaged, and the maximum amplitude of the peak response was recorded (peak amplitude; SEP) (Figure 4) and used to calculate mean, SEM, and median SEP values (Table S2).

**Statistical Analysis.** We used the Illumina BeadStudio software to analyze the gene expression data. Data from affected individuals were compared with data from control samples in a two-group differential expression using the Illumina rank invariant normalization and custom error model. For quantitative PCR, a linear mixed-models analysis was used to estimate marginal means for  $\Delta C$  of wild-type, homozygote, and heterozygous samples and differences of marginal means for wild type vs. homozygotes vs. heterozygotes (SAS 9.2; SAS Institute). The 95% confidence intervals and *P* values were calculated with Tukey–Kramer adjustment for multiple testing. The linear mixed models analysis with Tukey–Kramer adjustment for multiple testing also was used to estimate the marginal mean for the DIAPH3/GAPDH ratio as measured by band density on immunoblots. For luciferase assays, significance was determined with an unpaired *t* test. For SEPs in *Drosophila*, statistical significance was calculated by nonparametric Mann–Whitney analysis of median peak amplitudes using GraphPad Prism v5.0b statistical software (GraphPad Software).

**ACKNOWLEDGMENTS.** We thank the family for their participation, James Chang for technical assistance, and the University of Michigan Center for Statistical Consultation and Research for statistical support for the quantitative RT-PCR and immunoblotting experiments. We thank Henry Higgs (Dartmouth Medical School) for providing the DT154 anti-DIAPH3 antibody, Mark Peifer (University of North Carolina) for providing UAS-diaCA flies, Azusa Kamikouchi (Cologne, Germany) for providing JO1-Gal4, JO2-Gal4, JO3-Gal4, and JO4-Gal4 flies, Daniel Eberl (University of Iowa) for providing JO15/TM35b flies, and Jerry Yin (University of Wisconsin) for providing *w*<sup>118(isoCJ1)</sup> flies. This work was supported by National Institutes of Health Grants R01 DC007380 (to M.M.L.) and T32 DC000011-31 (to C.J.S.) and a grant from the Children's Hearing Institute of New York (to F.H.).

- Starr A, Picton TW, Sininger Y, Hood LJ, Berlin CI (1996) Auditory neuropathy. *Brain* 119:741–753.
- Lynch ED, et al. (1997) Nonsyndromic deafness DFNA1 associated with mutation of a human homolog of the *Drosophila* gene *diaphanous*. *Science* 278:1315–1318.
- Bione S, et al. (1998) A human homologue of the *Drosophila melanogaster diaphanous* gene is disrupted in a patient with premature ovarian failure: Evidence for conserved function in oogenesis and implications for human sterility. *Am J Hum Genet* 62:533–541.
- Waller BJ, Alberts AS (2003) The formins: Active scaffolds that remodel the cytoskeleton. *Trends Cell Biol* 13:435–446.
- Kim TB, et al. (2004) A gene responsible for autosomal dominant auditory neuropathy (AUNA1) maps to 13q14-21. *J Med Genet* 41:872–876.
- Starr A, et al. (2004) A dominantly inherited progressive deafness affecting distal auditory nerve and hair cells. *J Assoc Res Otolaryngol* 5:411–426.
- Grati FR, et al. (2009) Pure monosomy and pure trisomy of 13q21.2-31.1 consequent to a familial insertional translocation: Exclusion of PCDH9 as the responsible gene for autosomal dominant auditory neuropathy (AUNA1). *Am J Med Genet A* 149A:906–913.
- Letovsky J, Dynan WS (1989) Measurement of the binding of transcription factor Sp1 to a single GC box recognition sequence. *Nucleic Acids Res* 17:2639–2653.
- Brand AH, Perrimon N (1993) Targeted gene expression as a means of altering cell fates and generating dominant phenotypes. *Development* 118:401–415.
- Somogyi K, Rørth P (2004) Evidence for tension-based regulation of *Drosophila* MAL and SRF during invasive cell migration. *Dev Cell* 7:85–93.
- Kaczynski J, Cook T, Urrutia R (2003) Sp1- and Krüppel-like transcription factors. *Genome Biol*, 10.1186/gb-2003-4-2-206.
- Sgourou A, et al. (2004) Thalassaemia mutations within the 5'UTR of the human  $\beta$ -globin gene disrupt transcription. *Br J Haematol* 124:828–835.
- Thein SL (2005) Genetic modifiers of  $\beta$ -thalassaemia. *Haematologica* 90:649–660.
- Hudder A, Werner R (2000) Analysis of a Charcot-Marie-Tooth disease mutation reveals an essential internal ribosome entry site element in the connexin-32 gene. *J Biol Chem* 275:34586–34591.
- Edward AD, Eisenmann KM, Matheson SF, Alberts AS (2010) The role of formins in human disease. *Biochim Biophys Acta* 1803 (2):226–233.
- Peng J, et al. (2007) Myeloproliferative defects following targeting of the Drf1 gene encoding the mammalian diaphanous related formin mDia1. *Cancer Res* 67:7565–7571.
- Wilkie AO (1994) The molecular basis of genetic dominance. *J Med Genet* 31:89–98.

